Highly-performing and low-cost nanostructured membranes based on Polysulfone and Layered Doubled Hydroxide for high-temperature proton exchange membrane fuel cells

Authors.

Cataldo Simari, Ernestino Lufrano, Adele Brunetti, Giuseppe Barbieri, Isabella Nicotera:

2020

Peer-reviewed and accepted for publication in:

Journal of Power Sources, 2020, 471, 228440

https://doi.org/10.1016/j.electacta.2021.138214

Highly-performing and low-cost nanostructured membranes based on Polysulfone and Layered Doubled Hydroxide for high-temperature proton exchange membrane fuel cells

Cataldo Simari [1], Ernestino Lufrano [1], Adele Brunetti [2], Giuseppe Barbieri [2], Isabella Nicotera [1]

[1] *Department of Chemistry and Chemical Technologies, University of Calabria, 87036 Rende (CS), Italy*

[2] *Consiglio Nazionale delle Ricerche, Istituto per la Tecnologia delle Membrane, Via P. Bucci cubo 17C c/o Università della Calabria 87036 Rende (CS), Italy*

Abstract

The low cost, reduced fuel crossover and ease of preparation make sulfonated Polysulfone (sPSU) a potential candidate to replace Nafion electrolyte in proton exchange membrane fuel cells (PEMFCs). To reach a satisfactory proton conductivity the general strategy involves the preparation of macromolecules with high ion exchange capacity (IEC), even at the cost of sacrificing their mechanical properties. In this study, sPSU with relatively low IEC was used as polymer matrix for the preparation of nanocomposite electrolytes by dispersing Mg/Al-NO_3^- Layered Double Hydroxides (LDH). sPSU-LDH membranes were prepared by solution intercalation method and characterized by XRD, TGA and DMA, whereas water dynamics and proton conductivity were investigated by NMR (PFG and T_1) and EIS spectroscopies, respectively. The complete exfoliation and nanodispersion of the LDH platelets into the polymer enhance the thermo-mechanical resistance, the dimensional stability and the water retention capacity of the electrolytes. The formation of highly connected ion channels promotes an effective Ghrotthus-type mechanism for the proton transport also under dehydrating environment. Such features allowed proton conductivity values and electrochemical performances in single cell PEMFC distinctly higher than the Nafion recast, demonstrating the possibility to prepare cost-effective and high performing sPSU-based membranes able to operate under low-humidification and high temperatures conditions.

Keywords: Nanocomposite membranes; clays; LDH; polysulfone; PFG-NMR; proton transport.

1. Introduction

Polymer Electrolyte Membrane Fuel Cells (PEMFCs) have emerged as promising solution for clean, safe and efficient generation of electric power via chemical reaction. Unfortunately, current devices are still far from the large scale utilization since typically operate at low temperatures (60-80 °C) and require efficient thermal and water managements, which dramatically enhance the costs and the complexity of the system [1]. In dehydrating environment, that is high temperature and reduced relative humidity (RH) levels, Nafion® polymer (the state-of-the-art proton exchange membrane - PEM), fails to maintain its proton conductivity, dimensional stability, and mechanical integrity, leading to failure in the cell performances [2–5]. Nevertheless, it was demonstrated that improved reaction rate at both electrodes, easier thermal and water management and enhanced carbon monoxide tolerance of the platinum catalyst at the anode could be achieved by increasing the operating temperature of the device [6,7]. Accordingly, the development of polymeric membranes capable to operate under high temperature and anhydrous conditions has become the most compelling challenge to increase the chance of practical application of PEMFC systems[8,9].

To reach the goal, different alternatives was proposed [6] such as: (i) modification of per-fluorinated membranes by addition of hydrophilic and/or proton conductor fillers [10–12], (ii) synthesis of perfluorinated sulphonic acid polymer with short-side chain (SSCA-PFSA) [13,14], (iii) preparation of acid-base blends [15,16], (iv) modification of non-fluorinated polymers (nFPs) and preparation of related composite [17]. Due to the low cost, the remarkable chemical and mechanical resistance and the low permeability to the fuel of aromatic polymers [18,19], the latter approach is generally considered as one of the most encouraging toward the preparation of alternative PEMs. However, pristine macromolecules are mostly hydrophobic and poor proton conductor. Therefore, great effort has been devoted on the suitable functionalization of nFPs. In this regard, very promising results were obtained on the sulfonated derivatives of poly(arylene ether)s [20], Polysulfone [21], polyether sulfone [22], poly(arylene sulfide sulfone nitrile)[23] and poly (ether ether ketone)[24]. In all these cases, however, satisfactory proton conductivity were achieved only at high IEC values, with consequent excessive water uptake, remarkable dimensional variation and unsuitable mechanical properties [17,25,26], which made the resulting membranes inadequate for PEMFCs applications. Basically, a clear trade-off effect between conductivity properties and structural stability exists. To avoid these problems, the incorporation of a proper filler inside the polymer matrix proves a facile and effective approach to enhance the proton conductivity and at the same time improves the membrane robustness. It was demonstrated, for example, that the addition of inorganic fillers, such as SiO_2, TiO_2, ZrO_2, phosphotungistic acid and zeolite nanoparticles, increase the water uptake and consequently the proton conductivity of the pristine polymer while maintaining adequate mechanical

strength of the resulting electrolyte [27–29]. In all these cases, however, due to the water evaporation from the membrane, a significant loss in proton conductivity generally occurs at elevated temperatures. At low hydration-state, in fact, high proton transfer efficiency could be achieved only if the acid sites of the nanofiller effectively connect the disordered conducting groups of the polymer matrix [30,31]. By considering such "bridge-like" role of the additives, 2D-nanomaterials, such as graphene oxide, clays, Layered Double Hydroxide and single layered materials, have some peculiar structural properties. For instance, they can be easily exfoliated to individual platelets resulting in extremely large surface area and high aspect ratio. This improves the interfaces properties between the additive and the polymer structure, which also leads to reduced fuel crossover, enhanced mechanical strength and, due to their hygroscopic nature, outstanding retention capacity inside the electrolyte membrane [32–35].

In this study, the sulfonated derivative of Polysulfone (sPSU) was selected as polymer matrix on account of its low cost, large availability, low environmental impact, excellent film-forming ability, and remarkable thermo-mechanical resistance [36]. Furthermore, the transport and structural features of sPSU can be easily tuned since a large number of synthetic strategies and sulfonating agents exist [21,37]. In our case, PSU sulfonation have been achieved according to the procedure proposed by Lufrano et al. [38], which involves the use of trimethylsilyl chlorosulfonate as sulfonating agent. Due to its mild sulfonation activity, the use of this agent allows to preserve the backbone structure from undesired degradation phenomena. Reaction was controlled at 50 °C for 6 h to reach an Ion Exchange Capacity (IEC) of circa 1.3 meq g^{-1}. Such low IEC value was selected to preserve the structural stability of the macromolecule, while suitable transport properties were ensured by the addition of a proper filler. Accordingly, sPSU composite membranes were prepared by dispersing Layered Double Hydroxides (LDH) nanoparticles, an anionic (or hydrotalcite-type) clay, in the polymer matrix. The chemical structure of the LDH is similar to brucite $Mg(OH)_2$, crystallize in a layer-type lattice and can be represented as $[M_{1-x}^{(II)} M_x^{(III)} (OH)_2]^{x+}[A^{m-}_{x/m}]\cdot nH_2O$, where $M^{(II)}$ is a divalent metal cation (Mg, Mn, Fe, Co, Ni, Cu, Zn, Ga) and $M^{(III)}$ is a trivalent metal cation (Al, Cr, Mn, Fe, Co, Ni, and La), while A^{m-} is an interlayer anion, such CO_3^{2-}, OH^-, NO_3^-, SO_4^{2-} or ClO_4^- [39,40]. Therefore, the layers have a fixed positive charge and neutrality is obtained by anions present in the galleries. The main features of this clay compared to other 2D-layered materials are the very high anion exchange capacity (maximum theoretical value is about 2.8 meq/g), easy synthesis and functionalization, high purity and effective control on particle size and crystallinity [41]. Additionally, some specific advantages include the swelling ability, water holding and high specific surface areas. Finally, LDHs demonstrated good chemical affinity with several polymers, including PFSA ionomers, facilitating its nanodispersion in order to prepare

nanocomposite materials with higher thermal and mechanical properties [42]. In particular, for this study, LDH based on Mg^{2+}/Al^{3+} (2:1 metals ratio) with NO_3^- interlayer anion was chosen and synthesized because it demonstrated a beneficial effect on the overall performance of Nafion-based nanocomposites [43]. Whereas, nanocomposites based on the dispersion of LDH particles in non-fluorinated polymers is a quite unexplored route. Kim and co-workers firstly reported the preparation of sPEEK-LDH nanocomposite membranes with increased thermal stability and proton conductivity compared to pristine sPEEK [44]. Similarly, Herrero et al. demonstrated the introduction of LDH particles clearly enhances the electrical and transport features of sPSU membranes.[45] However, none of the previous studies provided any real PEMFC application with MEA.

In the present work, sPSU-LDH nanocomposite membranes with different filler loading were prepared by a simple solution intercalation method. The degree of exfoliation of the LDH particles and the structure of the composite membranes has been investigated by X ray diffraction, while the thermogravimetric analysis and dynamic mechanical analysis allowed the complete characterization of their thermal and mechanical behaviour, respectively. Based on the water uptake behaviour and water molecular dynamics inside the membranes we attempted to propose a reasonable microstructure of the ionic cluster that fit the observed properties. NMR spectroscopy has been widely used to study the proton transport properties by the direct measurements of the self-diffusion coefficients (Pulse Field Gradient NMR method) and by relaxation times (T_1) measurements to investigate on the short-range mobility. Proton conductivities have been assessed by electric impedance spectroscopy in a wide range of temperatures and humidification conditions. As a final point, the single H_2/O_2 fuel cell performances of the electrolytes were also investigated. Outstanding results were obtained on cell assembled with sPSU-LDH_3 films, for which remarkable power density was achieved under high temperature and very low relative humidity.

2. Experimental

2.1 Materials and chemicals

Commercial Polysulfone (Lasulf) was supplied by Lati SPA (Varese, Italy). Chloroform, trimethylsilyl chlorosulfonate, sodium methoxide/methanol solution, ethanol and *N*,*N*-dimethylacetamide (DMAc) were all purchased by Aldrich and used as received.

2.2 Synthesis of sPSU and LDH

The sulfonation of Polysulfone was carried out according to the procedure described elsewhere by Lufrano et al. [46]. Briefly, PSU was first dried and thus dissolved in anhydrous chloroform at room

temperature. The resulting solution was treated with trimethylsilyl chlorosulfonate (molar ratio of sulfonating agent/repetitive units equal to 2.5) for 6 h at 50 °C under reflux to obtain the silyl polysulfonate derivative. After reaction was completed, sodium methoxide solution was used to cleave the silyl sulfonate moieties over 1 h to yield the sulfonated Polysulfone in sodium form (which is more stable). This latter was isolated from the solution by precipitation in a bath of ethanol. The resulting powder was recovered by filtration, vigorously washed with ethanol and rinsed several times with deionized water prior to be heated at 60 °C in an oven till dryness.

LDH has been prepared by co-precipitation of Mg^{2+} and Al^{3+} salts, according to the procedure described elsewhere [22]. For the synthesis, performed under nitrogen gas flow, 100 mL of a solution of $Mg(NO_3)_2 \cdot 6H_2O$ (0.05 mol), $Al(NO_3)_3 \cdot 9H_2O$ (0.025 mol) and $NaNO_3$ (0.045 mol) salts was prepared and drop-wise added to an aqueous solution of NaOH (2.5 M) until pH 10. The resulting dispersion was vigorously stirred at 60 °C for 24 h, prior to be separated by centrifugation, washed with water and finally dried in an oven at 80 °C for 24 h. For this study, the Mg^{2+}:Al^{3+} metal ratio was fixed to 2:1.

2.3 Membranes preparation

For pristine membranes, the appropriate amount of sulfonated Polysulfone was dissolved in DMAc (10% wt. solution) at room temperature until clear and homogeneous solution was obtained. The solution was then cast on a petri dish and dried in oven at 60 °C until complete evaporation of the solvent. To prepare composite membranes, LDH was first dispersed in DMAc during 24 h by alternating vigorous mechanical stirring with ultrasonication. This dispersion was then added to a sPSU solution in DMAc and left under stirring at room temperature for additional 24 hours. The amount of LDH particles incorporated in the membrane was from 2 to 5 % by weight with respect to the polymer. The composite electrolytes were obtained by casting the resulting sPSU-LDH dispersions on a petri dish and heating in oven at 60 °C till dryness. Finally, both pristine and composite membranes were converted into the acid form by soaking them in 1M H_2SO_4 solution (7 h at 50-60 °C), followed by washing several times with boiling deionized water to remove any residual acid.

Nafion recast membrane was fabricated through a solvent casting method as referential sample. Briefly, 1 g of Nafion perfluorinated resin solution (20 wt % in mixture of lower aliphatic alcohols and water, from Aldrich) was heated at about 60 °C till dryness and thus re-dissolved in 10 mL of DMF until a clear solution was obtained. The resulting solution was cast on a Petri dish and dried in the oven at 60 °C until the solvent was completely evaporated. Finally, the membranes was thermally and chemically activated according to a standard procedure.[30] The dry thickness of all the

prepared membranes was circa 50 ± 5 μm. Figure 1 shows the photos of the four polymer electrolyte membranes prepared in this study. With the exception of the sample containing 5 wt% of LDH (sPSU-LDH$_5$), all the membranes appear completely transparent. In fact, no clay particles crystals are observed in both sPSU-LDH$_2$ and sPSU-LDH$_3$ samples suggesting the absence of agglomerates or inhomogeneity. Instead, the white-yellowish appearance of sPSU-LDH$_5$ membrane is likely due to some particles clustering or agglomeration.

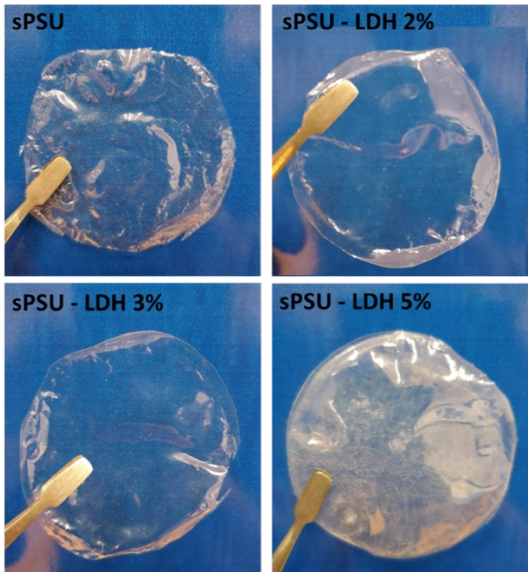

Figure 1. Pictures of pristine sPSU and sPSU-LDH composites (at 2, 3 and 5% of filler loading) membranes.

2.4 Instrumental characterization

XRD patterns, recorded in the 2θ range from 2 to 60°, were acquired with a X'Pert 3710 X-Ray diffractometer (Philips, Eindhoven, The Netherlands) using a Cu-Kα source operating at 40 kV and 20 mA. Thermogravimetric analysis (TGA) were carried out on approximately 8 mg of each sample using a Perkin-Elmer TGA-6 instrument in the range 25-800 °C at a scan rate of 5 °C min^{-1} under N_2 flux (16 mL min^{-1}). Dynamic Mechanical Analysis (DMA) measurements were performed on a Metravib DMA/25 analyzer equipped with a shear jaw for films clamping. A dynamic stress of amplitude 10^{-4} at 1 Hz is applied on a rectangular shaped sample, in the temperature range 25 - 250 °C, with a heating rate of 2 °C min^{-1}.

2.5 Ion Exchange Capacity (IEC) and water uptake

Conventional titration method was used to determine the Ion Exchange Capacity (IEC) of the sPSU-based membranes [47]. Samples in acid form were immersed in 2M NaCl solution for 24 h at room temperature to completely release H^+ via exchanging with Na^+. The amount of released H^+ was

titrated with standard NaOH solution (0.1 M), using phenolphthalein as an indicator. The IEC values (meq g^{-1}) was calculated according to:

$$IEC = \frac{M_{(NaOH)}\ V_{(NaOH)}}{W_{dry}};\ meq\ g^{-1} \qquad (Eq.\ 1)$$

where V is the volume (mL) and M the concentration (mol/L) of the NaOH solution consumed to neutralize the H^+ ions, while W_{dry} is the dry weight of the sample.

From the difference between the wet and dry mass of each membrane the water uptake (w.u.) was determined. A piece of dry sample was weighted (m_{dry}) and swelled in distilled water for 24 h at 20 °C and at higher temperatures (from 30 to 80 °C each 10 °C) for 2 h. The membrane was then removed, wiped with blotting paper to eliminate surface water droplets and quickly measured (m_{wet}). The procedure has been repeated five times for each sample, with an error of *circa* 2%. The w.u. was calculated by the following Eq. 2:

$$w.u. = \frac{m_{wet} - m_{dry}}{m_{dry}} * 100;\ \ \% \qquad (Eq.\ 2)$$

From the water content and the IEC the number of water molecules per -SO_3H group, defined as λ value, can be calculated by the formula reported in Eq. 3:

$$\lambda = \frac{\text{w.u.}}{\text{IEC} * \text{M}_\text{w}} \qquad (Eq.\ 3)$$

where, M_w is the molecular weight of water (18.01 g mol^{-1}).

2.6 NMR (PFG and relaxometry) spectroscopy

The ^{1}H-NMR measurements were performed on a Bruker AVANCE 300 wide bore spectrometer working at 300 MHz on ^{1}H and equipped with a Diff30 Z-diffusion 30 G/cm/A multinuclear probe with substitutable RF inserts. Pulsed field gradient stimulated-echo (PFG-STE) technique [48] was used to directly measure the self-diffusion coefficient (D). This particular sequence allows to measure D in materials characterized by transverse relaxation time (T_2) considerably shorter than the longitudinal relaxation time (T_1) and foresees three 90° RF pulses ($\pi/2$-τ_1- $\pi/2$- τ_m- $\pi/2$) with two gradient pulses applied after the first and the third RF pulses. At time $\tau = 2\tau_1 + \tau_m$ the echo is found. The FT echo decays were analysed by means of the relevant Stejskal–Tanner expression (Eq. 4):

$$I = I_0 e^{-\beta D} \qquad (Eq.\ 4)$$

with I and I_0 representing the intensity/area of a selected resonance peak with and without gradients, respectively, D the self-diffusion coefficient and β the field gradient parameter. This latter is defined by Eq. 5:

$$\beta = [(\gamma g \delta)^2(\Delta - \frac{\delta}{3})] \qquad (Eq.\ 5)$$

where g, δ and Δ are the amplitude, duration, and time delay of the gradient field, respectively. For the measurements δ and Δ were kept at 0.8 and 8, respectively, while g ranged between 200- 800 G cm^{-1}. For the self-diffusion measurements an uncertainty of ~3 % was calculated. Additionally, the inversion recovery sequence (π-τ-π/2) was used to investigate the spin-lattice relaxation times (T_1). The detailed experimental procedure to prepare the NMR sample is described elsewhere [49,50]. Both D and T_1 were investigate in the range 20-130 °C, with steps of 20 °C and 15 minutes of equilibration time for each temperature.

2.7 Electrochemical Impedance spectroscopy (EIS)

The in-plane proton conductivity was determined by Electrochemical Impedance Spectroscopy (EIS) using a commercial four-electrode cell (BT-112, Scribner Associates Inc.) fitted between the anode and the cathode flow field of a fuel cell test hardware (850C, Scribner Associates Inc.). Temperature and relative humidity (RH) were controlled by the use of a humidification system (Fuel Cells Technologies, Inc.) directly connected to the cell. Here the measurements were performed under different temperature (30, 60, 90 and 120 °C) and relative humidity (30, 50 and 90) to simulate the wide operating condition that PEMFCs should withstand. A PGSTAT 30 potentiostat/galvanostat (Methrom Autolab) equipped with an FRA module was used to measure the AC impedance response of the cell. This latter was recorded at OCV in the frequency range between 1 Hz-1 MHz under an oscillating potential of about 10 mV. The impedance spectra were analyzed by NOVA software to extrapolate the electrolyte resistance (R_{el}) as the high-frequency intercept on the real axis of the Nyquist plot. From its ohmic resistance, the proton conductivity (σ) of the electrolytes were calculated according to Eq. 6:

$$\sigma = \frac{d}{R_{el} * A}; \quad \text{S cm}^{-1} \qquad \text{(Eq. 6)}$$

where *d* is the distance between the electrodes and *A* is the active surface area.

2.8 Fuel Cell test

For the H_2/O_2 fuel cell test, electrodes were manufactured by casting knife technique as described by Baglio et al. [51]. The catalytic ink was prepared by mixing under sonication the commercial

platinum (Pt/C, 40% supported on carbon - Alfa Aesar) with 33% of Nafion ionomer (20% ionomer solution – Ion Power). After the adequate dispersion was obtained, the catalytic ink was deposited onto the backing layer of a commercial Sigracet 25-BC Gas Diffusion Layer (SGL). A Pt loading of 0.5 mg cm^{-2} for both the anode and the cathode side was used. Membrane Electrodes Assemblies (MEAs) were obtained by hot pressing the electrodes onto the different membranes (recast Nafion and Nafion 212 benchmarks, and sPSU-based membranes) at 130 °C and 30 kg cm^{-2} for 2 min. The investigation of films with comparable thickness (ca. 50 μm) allowed a more accurate comparison among of the resulting cell performances. For the polarization experiments, galvanostatic measurements were carried out under steady-state conditions by connecting the cell to a home-made test bench equipped with an electronic load (Fideris, 125W, 20 V, 5 A). The MEAs were tested in a 5 cm^2 single cell in the temperature range 80-110 °C, feeding 200 mL min^{-1} of hydrogen and oxygen to the anode and cathode, respectively, at atmospheric pressure and varying the RH at the anode from 100 till 25 %. Reactants feed flow rates were maintained constant during the experiments. Mass flow controllers (Brooks Instruments) were used to control the feed flow rate on either side of the cell, while the temperature and RH of the cell were measured by appropriate sensors.

3. Results and Discussion

3.1. Structural and thermal properties

The XRD patterns of Mg/Al-NO_3^- LDH powder, pristine sPSU and the sPSU-LDH composite membranes with different LDH loading (2, 3 and 5 wt%) are illustrated in Figure 2a. The XRD profile of the LDH powder exhibits a main diffraction peak at 2θ = 10.1°, which corresponds to a basal spacing (d_{003}) of 9 Å [43,52]. The absence of this peak in the membranes with 2% and 3% of filler indicates that the platelets lost their stacking, thus confirming that completely exfoliated nanocomposite membranes have been achieved. This is amenable to the favourable electrostatic interactions occurring between the positively charged LDH platelets and the structure of sPSU (which is negatively charged). Despite this, upon increase of the LDH content at 5% two weak and sharp diffraction peaks (evidenced by the arrows) appear. The first one, at 2θ of *circa* 10° clearly corresponds to the d_{003} diffraction peak of LDH stacked particles, while the second one likely results from the intercalation of the polymer chains in the interlayer space of some LDH particles [53,54].

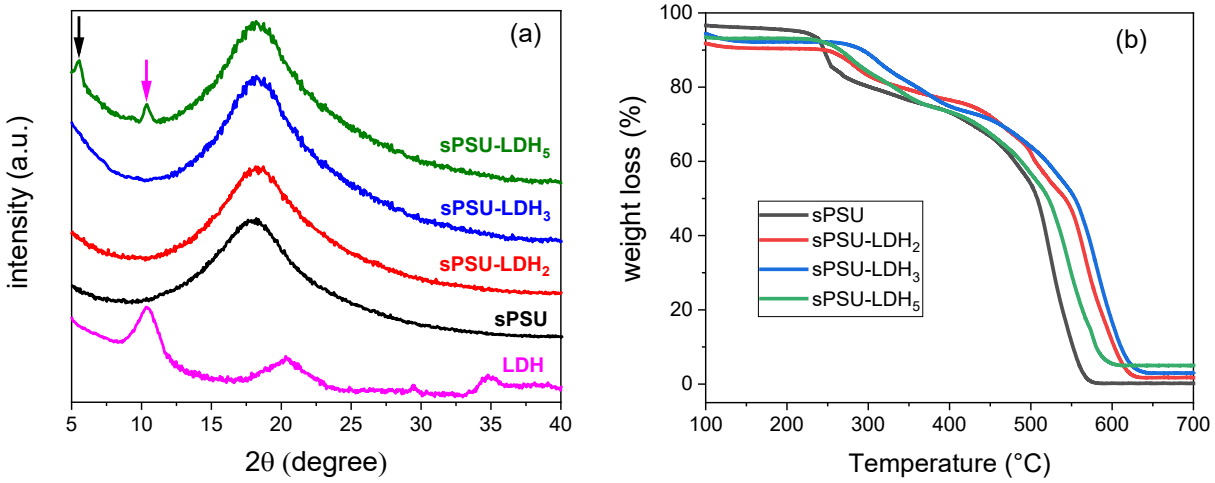

Figure 2. (a) XRD patterns of Mg/Al-LDH powder, sPSU and sPSU-LDH nanocomposites membranes; (b) Thermogravimetric analysis of the membranes.

Satisfactory thermal and mechanical resistances of the electrolyte membrane are two of the main requirements for the long life of the cell. Accordingly, TGA and DMA tests were carried out to investigate the effect of the LDH platelets on the thermo-mechanical stability of the resulting film. Figure 2b shows the thermogravimetric analysis of sPSU and composite samples in the temperature range 100-700 °C. The TGA pattern of sPSU shows two main degradation steps: the first one taking place between 200 and 400 °C is amenable to decomposition of sulfonic acid (-SO_3H) groups; while the degradation of the polymer backbone starts above 400 °C. The presence of nanoplatelets leads

to a significant upward shift of both degradation steps, indicating an improvement of the thermal resistance of the membranes. The residual amount at 700 °C visible in the nanocomposite membranes is assigned to the inorganic structure of the LDH particles. Therefore, the strong variation on the TGA patterns of composite electrolytes with respect to neat sPSU suggest the effective particles dispersion inside the hosting matrix [35,55].

The positive effects of the LDH material on the thermal and mechanical stability of the final membrane were further confirmed by the dynamic mechanical analysis (DMA) results. Figure 3 shows the enlarged details, from 120 to 240 °C, of the temperature evolution of storage modulus and dumping factor (tan δ) of the membranes. The addition of LDH platelets in the sPSU matrix results in a marked increase in the storage module and a considerable extension of the thermal resistance. In fact, the moduli of composite sPSU-LDH membranes remain quite constant even at very high temperatures, proving how these membranes are able to maintain outstanding mechanical strength (e.g., 800 MPa for sPSU-LDH$_3$ sample) without dimensional changes and physical deterioration up to 220 °C. The dumping factor plot showed in Figure 3b better elucidates the relationship between thermal resistance and LDH content. Tan δ profile is characterized by a single peak in the high temperature region which is generally assigned to the α transition (T_g) of the polymer's ionic clusters. This polymer transition is shifted at higher temperatures by increasing the filler content, up to reaches 225 °C with 3 wt% of loading. Compared to the typical T_g of the Nafion ion clusters which is about 140 °C, [30], the proposed composite membranes can provide significantly higher mechanical strength and greater thermal stability: sPSU-LDH can definitively withstand high operating temperatures and severe stress conditions.

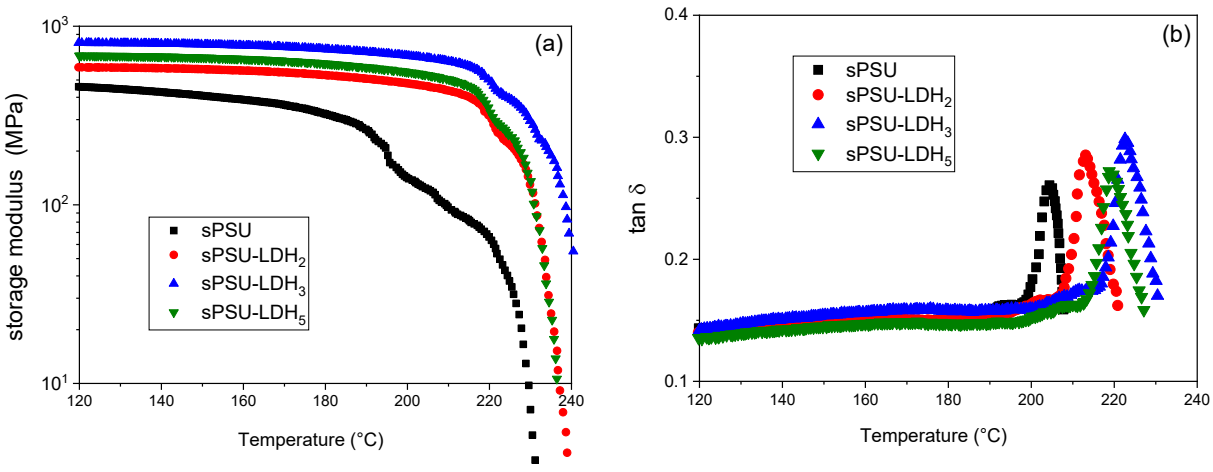

Figure 3. (a) Storage modulus and (b) Tan δ of the sPSU-based membranes as a function of the temperature.

3.2 IEC and water uptake behaviour

Figure 4 shows the IEC and the water uptake values for sPSU-based composite membranes as a function of the filler amount. Membrane's IEC grows with increasing LDH content reaching the value of 1.49 meq g^{-1} at 3 wt% of filler loading due to the charged nature of the anionic lamellae dispersed inside the sPSU matrix. Actually, by considering the Anion Exchange Capacity (AEM) of the synthetized LDH, which is about 2 meq g^{-1}, the considerable increasing of the final IEC of the composite membrane is justified by the exfoliation of the clay material in the polymer.

At higher filler loadings (5 wt%), a reduction of the IEC emerges. Here, as revealed by the XRD analysis, most of the LDH particles are not exfoliated (platelets keep their stacking) in the sPSU-LDH_5 sample, decreasing, as consequence, the number of hydrophilic sites available for proton exchange.

What discussed is expected to strongly affect the water absorption capacity of the electrolytes. Indeed, it is generally assumed that a variation in the IEC results in a great alteration of the water absorption capacity [56]. In these membranes, however, there are no significant variations of water uptake with the filler loadings, and so with the IEC: it varies between 27 wt% of the pristine sPSU and the 30 wt% of the sPSU-LDH_3. This implies that the PSU polymeric matrix does not allow excessive swelling of the membranes, i.e. there is little free volume that can gradually accommodate large quantities of water. Such outcome is still positive because it guarantees the dimensional stability of the electrolyte membrane during the PEMFC operation. Indeed, it is well known that strong variation in the water content under operation condition, could lead to over-swelling, deterioration of mechanical resistance and, most important, to dimensional mismatch when the membrane is assembled into a fuel cell [57].

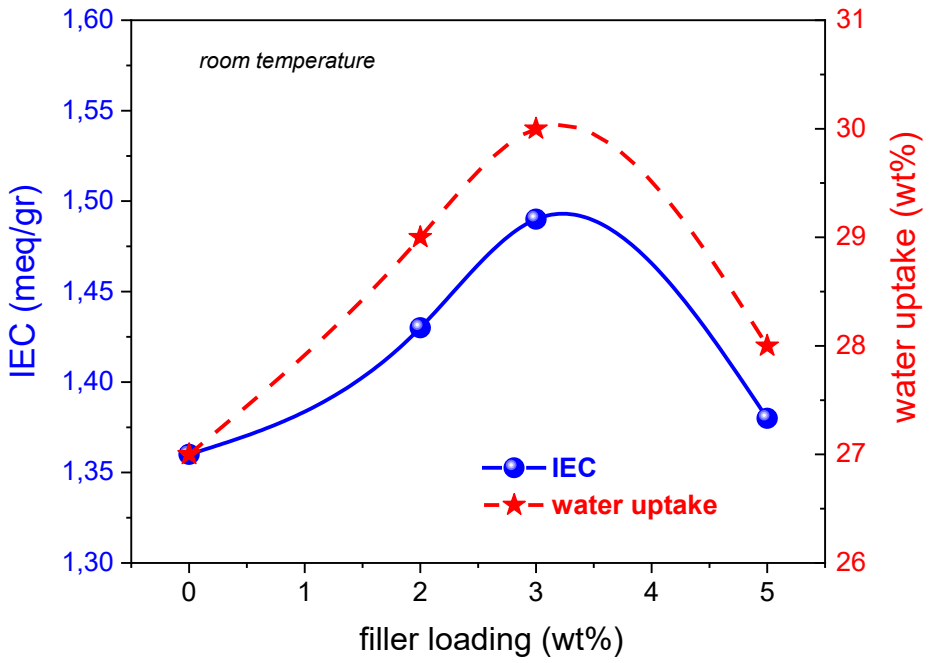

Figure 4. Ion exchange capacity and water uptake values at different filler loadings in the sPSU/LDH composite membranes.

To gain insight about the hydrolytic resistance of the membranes their swelling behavior under variable temperature was also investigated. Figure 5 shows the water uptake and the number of water molecules per mole of acid group (coordination number, λ) in the temperature range 20 - 80 °C. Compared with pristine sPSU, the dimensional resistance of the nanocomposite electrolytes slightly improves with 2 and 5 wt% of filler loading, and reaches the maximum stability in the sPSU-LDH_3 membrane, for which the water uptake barely rises from 30 % at 20 °C till 32 % at 80 °C, showing an excellent anti-swelling ability. From the λ values (Figure 5b), crucial information concerning the microstructure of the electrolyte films can be obtained. At 20 °C, λ is about 11 and is invariable with the filler loading, meaning that, although the IEC varies, the addition of LDH particles does not alters the microstructure of the ionic clusters (such as shape and size) but rather leads to a rearrangement in the distribution of the water molecules. It can be stated that as a result of the dispersion of LDH particles, the amount of bulk water decreases because most of the H_2O molecules interact with the surface of the anionic lamellae.

The number of water molecules per mole of acid groups gradually raises with the temperature, reaching, at 80°C, values of 15 for pristine sPSU, 13.5 for sPSU-LDH_2 and 14.5 for sPSU-LDH_5, but only 12 for PSU-LDH_3 film. Therefore, if the dimensions of the hydrophilic domains increase with the temperature increasing, allowing the absorption of larger amount of water, for the latter membrane seems that the temperature does not affect the cluster size. We can affirm that structural organization of the exfoliated filler in the sPSU-LDH_3 composite allows the right arrangement of

the water molecules, likely on the wide active surface of the nano-lamellae, without clusters swelling.

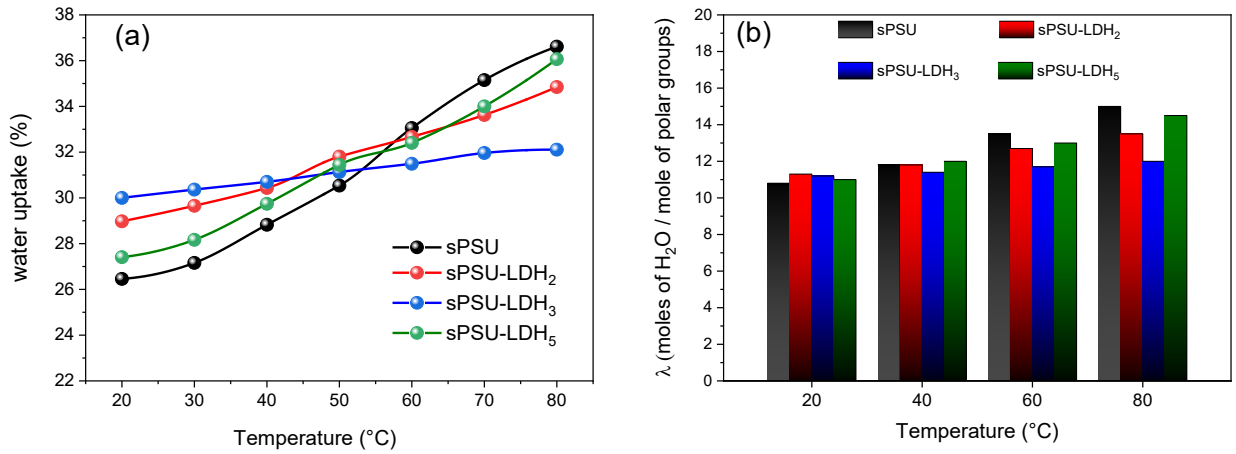

Figure 5. Temperature evolution of (a) water uptake and (b) λ for pristine sPSU and sPSU-LDH composite membranes.

3.3. Proton transport properties (D and T1)

^{1}H-NMR spectroscopy allowed to investigate the molecular dynamics (both long- and short- range) of water confined inside the hydrophilic clusters of the prepared electrolytes, through the direct measurements of the water self-diffusion coefficients (D) and the longitudinal relaxation times (T_1), respectively.[58,59] Figure 6a shows the water self-diffusion coefficients measured on the swelled membranes (at the maximum water uptake) in the temperature range 20-130 °C. At low temperatures, 20-60 °C, there is no significant discrepancy of D among the membranes, likely due to the similar water uptakes. Above 60 °C, the diffusivity behaviour of each sample starts to sharply diverge: (i) pristine PSU shows a gradual decreasing of D to the point that, at 130 °C, is one order of magnitude lower than the initial ones; (ii) the presence of LDH slows down this process of collapse of diffusion at increasingly higher temperatures; (iii) remarkable profile of sPSU-LDH$_3$ sample, for which D increases up to 120 °C and then remains almost stable at 130 °C. The decrease of D is due to the evaporation of a fraction of the bulk-water from the membrane, that is, of those water molecules "freer" from electrostatic interactions. In this regard, the LDH lamellae in the polymer matrix are able to retains a suitable amount of water at very high temperature, with no need of external humidification system. However, these results demonstrate how it is not only the nature of the filler to determine the effectiveness of the final nanocomposite, but rather how it is organized within the polymer and the kind of nanostructure created. For instance, the composite with 3 wt%

of LDH shows proton diffusion at 130 °C, over 1 order of magnitude higher than the other two composite membranes.

The analysis of spin-lattice relaxation times (T_1) allows to complete the pictures about the structural organization of water inside such complex systems. With respect to D, T_1 refers about the short-range translational and rotational motions on a time scale comparable to the inverse NMR frequency (~1 ns), and can be ascribed to the energy transfer rate from the spin system to the neighbouring molecules (the lattice). In a nutshell, the larger the interactions between spin and lattice, the quicker the relaxation (shorter T_1), with T_1 generally increasing with the temperature [60]. In Figure 6b we can observe the shorter T_1 values for the composite membranes, because a larger amount of bound water is present. Among them, the lowest values result for the sPSU-LDH_3 sample, meaning that here water molecules are experimenting the highest electrostatic interactions with the lattice (polymer and filler). On the contrary, pristine PSU membrane manifests the higher relaxation times up to 80 °C followed by a sharp drop, so free/bulk water that easily evaporates above this temperature. Finally, while in composites at 2 and 5 wt% of filler loading we observe a slightly decreases of T1 above 100 °C, in sPSU-LDH_3 film it constantly increases for the entire temperature range. Such evidence indicates that the structuring/arrangement of the water molecules in this membrane does not change with the temperature. It is in agreement also with the invariability of λ discussed above.

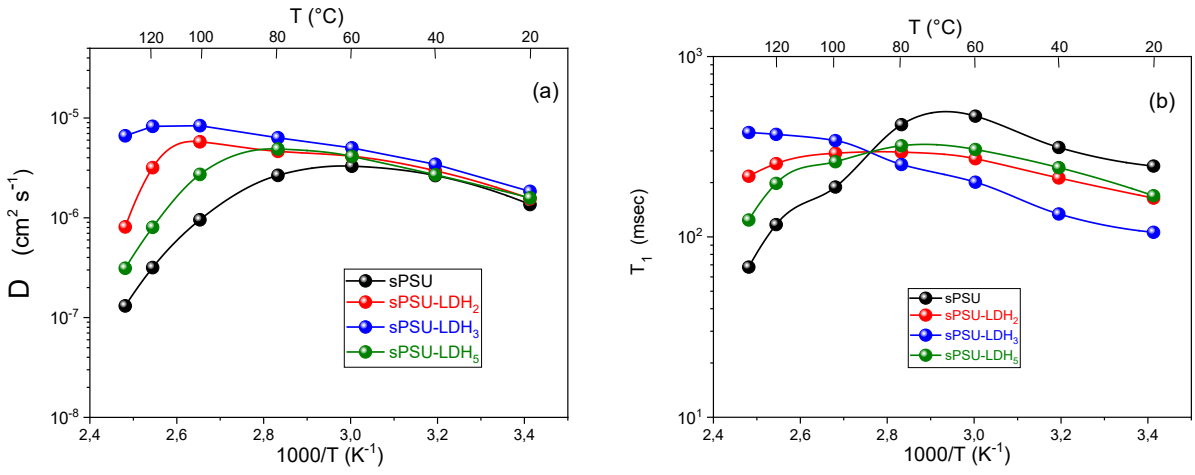

Figure 6. (a) Self-diffusion coefficients and (b) T_1-relaxation times as a function of the temperature (from 20 °C to 130 °C) of the water confined in sPSU-based membranes.

3.4. Proton conductivities (EIS)

The Arrhenius plot of the proton conductivity (σ) measured on the sPSU-based electrolyte membranes are shown in Figure 7 for three different relative humidity, i.e., 90, 50 and 30%. For comparison σ values of recast Nafion have been also reported. As expected, the proton conductivity of pristine sPSU is evidently lower than that of Nafion. In contrast to Nafion's microstructures, the weaker acidity of the sPSU polymer and the lower microphase separation between the hydrophilic and hydrophobic domains lead to narrower and less interconnected hydrophilic ion channels. The phenomenon is well described for other sulfonated hydrocarbon polymers [61] and has obviously a detrimental effect on the proton transport properties. The appropriate nanodispersion of a filler such as this LDH material allows achieving a significant enhancement of σ so that the composite at 3 wt% of filler loading reaches values almost comparable with those of Nafion. Even under low-hydration conditions (RH = 30%), which is an important requirement for the development of PEMFCs able to operate at high temperature, the conductivity of sPSU-LDH_3 membrane exceeds that of Nafion. This is a noteworthy result if we consider that the proton mobility of hydrocarbon-based polymer electrolytes is generally not suitable for practical application in PEMFCs [22].

By taking into account the NMR results, we can certainly state that the dispersion of LDH platelets inside the sPSU matrix favours the retention of a large number of water molecules which promote an effective proton transport through the formation of highly connected proton paths. The effective Ghrotthus-type mechanism for the proton transport in such composite membrane is confirmed by the activation energies calculated from the Arrhenius plots and reported in Table 1. The sPSU-LDH_3 composite membrane shows values practically superimposable to those of the recast of Nafion, and in agreement with a *hopping-type* mechanism.

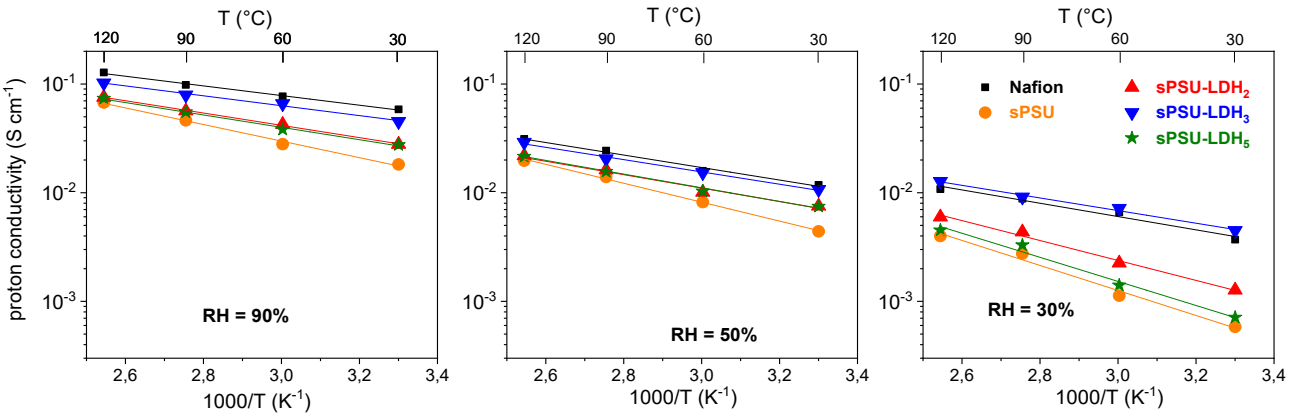

Figure 7. Arrhenius plots of proton conductivities at different RH% (90, 50 and 30%). The σ values of recast Nafion has been reported as benchmark. Solid lines represent the linear fitting to experimental data.

Table 1. *Activation energies of the proton conductivity (@ RH 90, 50 and 30 %) of both sPSU-based electrolytes and recast Nafion.*

Membrane	Activation Energy (kJ mol^{-1})		
	90% RH	50% RH	30% RH
Nafion recast	**8.48**	**11.01**	**11.71**
sPSU	14.62	16.63	22.03
sPSU-LDH$_2$	10.83	12.06	17.56
sPSU-LDH$_3$	**8.72**	**10.83**	**11.12**
sPSU-LDH$_5$	10.90	11.81	21.22

3.5. H_2/O_2 fuel cell tests under low-RH condition

MEAs prepared with PSU-based membranes were tested in a 5 cm^2 single cell PEMFC using hydrogen at the anode and oxygen at the cathode, both at pressure of 1 atm. Tests were performed at different operation conditions including at high temperature and reduced relative humidity, that is 80 °C / 30% RH and 110 °C / 25% RH, respectively, in order to evaluate the final performance of the new nanocomposite membranes and to meet the US DOE (Department of Energy) targets for high temperature PEMFCs. Polarization curves and power density behaviour of the pristine sPSU and sPSU-LDH$_3$ samples at the above harsh operating conditions, are showed in Figure 8. In the graphs, two Nafion membranes are also showed as references: Nafion recast membrane prepared for this study and a Nafion 212 commercial membrane chosen because has similar thickness (i.e. 50 μm). Besides, the main electrochemical parameters, such as OCV, potential and current density @ 0.6 V, and maximum current and power density, for all the samples were acquired and summarized in Table 2. The cell performances collected at higher relative humidity conditions are, instead, reported in Figure S1 of the Supporting Information.

The presence of LDH nanoparticles inside the sPSU matrix increases the open circuit voltage (OCV) indicating a reduction of the gas permeability through the electrolyte. MEA based on sPSU-LDH$_3$ membrane shows the highest OCV, with a value of 0.981 V against 0.891 V and 0.901 V supplied by the benchmarks recast Nafion and Nafion 212, respectively. This is amenable to the barrier properties of the phyllomorphous materials [62–64] that, following the complete exfoliation of the lamellae and the homogeneous dispersion, effectively hinders the H_2 crossover from the anode to the cathode. The PEMFC performance improves in the order sPSU< sPSU-LDH$_5$ < sPSU-LDH$_2$ < sPSU-LDH$_3$, with the same trend described for the proton conductivity properties. However, it is worth underline the peak power density of 254 mW cm^{-2} get with the sPSU-LDH$_3$ sample, which is over three times respect to the sPSU filler-free (74.4 mW cm^{-2}) and most important, about 30 %

higher than the maximum power dnsity registered for both the Nafion recast (197.4 mW cm^{-2}) and Nafion 212 (201.2 mW cm^{-2}). It is worth pointing out that the values recorded on the two Nafion benchmarks are in agreement with those typically reported in the literature.[65–67]

Such results demonstrate the high efficiency of such composite membrane, likely attributable not only to its higher proton conductivity but also to the better capacity to retain water under low-humidification conditions. Beside to the ohmic regions, differences were found also in the mass transport regions of the polarization curves: due to the lower H_2 crossover, sPSU-LDH_3 electrolyte yielded peak current density of 741.9 mA cm^{-2} @ 80 °C/ 30% RH, against 438.8 mA cm^{-2} and 648.6 mA cm^{-2} of sPSU and recast Nafion, respectively. Also under more drastic operating conditions, i.e. 110 °C and 25% RH, this electrolyte membrane showed the highest electrochemical performance. In fact, the poor ability to retain water of sPSU and Nafion membranes produces a conspicuous increasing of the ohmic resistance which reduces the cell performance. For instance, sPSU showed a decreasing of the maximum power density (35.9 mW cm^{-2}) of about 50% in these operating conditions. Similarly, both the Nafion PEMs exhibited a reduction of circa 40% (≈ 120 mW cm^{-2}), while the reduction of the sPSU-LDH_3 sample is of only about 20%, with a value of 204.5 mW cm^{-2}. To conclude, even if under high humidity conditions Nafion membranes are able to give good performance (see Fig. S1 of Supporting Information), only the high retention capacity of this sPSU-LDH composite membrane allows effective self-humidification even under dehydrating environment, and therefore allows the MEA to withstand high temperatures and low relative humidity without losing too much performance.

As further evidence of the above, an evaluation respect to other non-fluorinated membranes may also be useful. Therefore, in Table 1S of the Supporting Information, a comparison in terms of maximum power density between this sPSU-LDH composite membrane and several earlier published hydrocarbon-based PEMs, operating under similar experimental conditions (that is high temperature and/or low RH) is reported. Once again it demonstrates the remarkable performance of the sPSU-based membrane proposed in this work.

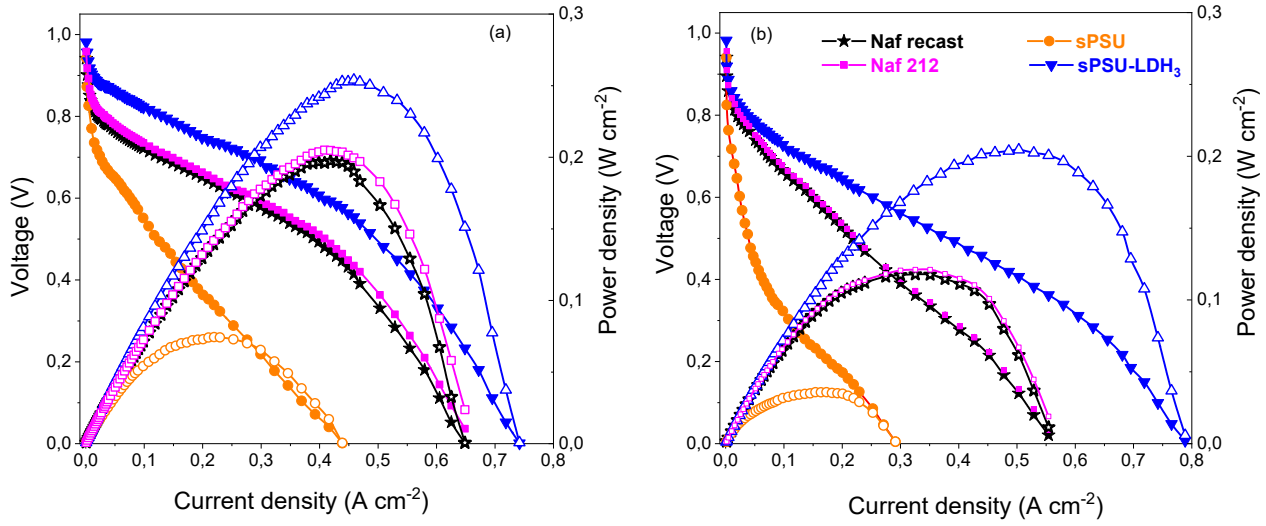

Figure 8. Polarization and power curves of H_2/O_2 PEMFCs at (a) 80 °C / 30% RH and (b) 110 °C/ 25% RH. The flux rates of H_2 and O_2 where both 200 mL min^{-1}.

Table 2. *Electrochemical parameters (Current density=CD and Power density = PD) of MEAs assembled with different membranes, under different operating conditions and 101 kPa abs H_2 /O_2.*

Membrane	80 °C 30% RH					110 °C 25% RH				
	OCV (V)	CD @ 0.6V (mA cm^{-2})	PD @ 0.6V (mW cm^{-2})	CD_{max} (mA cm^{-2})	PD_{max} (mW cm^{-2})	OCV (V)	CD @ 0.6V (mA cm^{-2})	PD @ 0.6V (mW cm^{-2})	CD_{max} (mA cm^{-2})	PD_{max} (mW cm^{-2})
Naf recast	0.891	275.4	167.4	648.6	197.4	0.887	149.7	92.7	554.3	117.8
Naf 212	0.901	278.6	169.7	649.2	201.2	0.890	157.5	93.5	558.9	121.1
sPSU	0.912	76.7	47.7	438.8	74.4	0.901	21.9	13.7	291.4	35.9
sPSU-LDH$_2$	0.935	285.5	172.0	605.1	176.2	0.914	127.3	76.4	485.9	109.9
sPSU-LDH$_3$	0.981	407.1	244.2	741.9	254.0	0.984	253.	151.5	788.5	204.5
sPSU-LDH$_5$	0.918	152.3	97.3	462.3	135.0	0.903	126.8	76.2	462.3	112.5

Conclusions

Nanocomposite sPSU-LDH membranes were prepared and characterized in terms of morphology, thermo-mechanical resistance, proton transport behavior and electrochemical properties. Sulfonation of Polysulfone (sPSU) was achieved by using trimethylsilyl chlorosulfonate as sulfonating agent, whereas Mg/Al (2:1) NO_3^- LDH material was synthesized by the co-precipitation method. Composite membranes at three filler loadings (2, 3 and 5 wt% with respect to the polymer) were prepared. XRD proved that only at the 3 wt% of loading the complete exfoliation of the LDH lamellae in the polymer matrix is obtained. Exfoliation and homogeneous dispersion of the nano-

platelets in the bulk polymer produce considerable improvement of the thermal and mechanical resistance, enhanced dimensional stability and beneficial effect on the transport properties of the final nanocomposite membrane, as demonstrated by NMR and EIS investigation. The sample sPSU-LDH_3 exhibits a proton conductivity of 13.7 mS cm^{-1} @120 °C / 30% RH, which is almost 30% higher than the Nafion recast used here as benchmark. The outstanding water retention ability of this composite electrolyte allows to get the best electrochemical performances in single cell PEMFC under low-humidification and high temperatures conditions, reaching a peak power density value of 204.5 mW cm^{-2} at 110 °C and 25% RH, that is twice the value reached by recast Nafion. The findings reveal the possibility to prepare cost-effective and high performing sPSU-based membranes able to effectively operate above 110 °C and reduced humidification.

Acknowledgements

This work was carried out with the financial support of the Italian Ministry of Education, Universities and Research (MIUR) by the ComESto Project: “Gestione aggregata di Sistemi di accumulo dell’energia in Power Cloud” (PNR 2015-2020).

References

[1] N.L. Garland, J.P. Kopasz, The United States Department of Energy's high temperature, low relative humidity membrane program, J. Power Sources. 172 (2007) 94–99. doi:10.1016/J.JPOWSOUR.2007.01.025.

[2] J. Yu, M. Pan, R. Yuan, Nafion/Silicon oxide composite membrane for high temperature proton exchange membrane fuel cell, J. Wuhan Univ. Technol. Mater. Sci. Ed. 22 (2007) 478–481. doi:10.1007/s11595-006-3478-3.

[3] M. Casciola, G. Alberti, M. Sganappa, R. Narducci, On the decay of Nafion proton conductivity at high temperature and relative humidity, J. Power Sources. 162 (2006) 141–145. doi:10.1016/j.jpowsour.2006.06.023.

[4] K.T. Adjemian, S. Srinivasan, J. Benziger, A.B. Bocarsly, Investigation of PEMFC operation above 100 °C employing perfluorosulfonic acid silicon oxide composite membranes, J. Power Sources. 109 (2002) 356–364. doi:10.1016/S0378-7753(02)00086-1.

[5] K. a Mauritz, R.B. Moore, State of understanding of nafion., Chem. Rev. 104 (2004) 4535–85. doi:10.1021/cr0207123.

[6] A. Chandan, M. Hattenberger, A. El-kharouf, S. Du, A. Dhir, V. Self, B.G. Pollet, A. Ingram, W. Bujalski, High temperature (HT) polymer electrolyte membrane fuel cells (PEMFC) e A review, J. Power Sources. 231 (2013) 264–278. doi:10.1016/j.jpowsour.2012.11.126.

[7] H. Zhang, W. Wu, J. Wang, T. Zhang, B. Shi, J. Liu, Enhanced anhydrous proton conductivity of polymer electrolyte membrane enabled by facile ionic liquid-based hoping pathways, J. Memb. Sci. 476 (2015) 136–147. doi:10.1016/j.memsci.2014.11.033.

[8] P. Xiao, J. Li, H. Tang, Z. Wang, M. Pan, Physically stable and high performance Aquivion / ePTFE composite membrane for high temperature fuel cell application, J. Memb. Sci. 442 (2013) 65–71. doi:10.1016/j.memsci.2013.04.014.

[9] M. Ji, Z. Wei, A Review of Water Management in Polymer Electrolyte Membrane Fuel Cells, Energies. 2 (2009) 1057–1106. doi:10.3390/en20401057.

[10] G.G. Kumar, A.R. Kim, K. Suk, R. Elizabeth, Nafion membranes modified with silica sulfuric acid for the elevated temperature and lower humidity operation of PEMFC, Int. J. Hydrogen Energy. 34 (2009) 9788–9794. doi:10.1016/j.ijhydene.2009.09.083.

[11] A. Saccà, I. Gatto, A. Carbone, R. Pedicini, E. Passalacqua, ZrO 2 – Nafion composite membranes for polymer electrolyte fuel cells (PEFCs) at intermediate temperature, J. Power Sources. 163 (2006) 47–51. doi:10.1016/j.jpowsour.2005.12.062.

[12] L.G. Boutsika, A. Enotiadis, I. Nicotera, C. Simari, G. Charalambopoulou, E.P. Giannelis,

T. Steriotis, Nafion?? nanocomposite membranes with enhanced properties at high temperature and low humidity environments, Int. J. Hydrogen Energy. 41 (2016) 22406–22414. doi:10.1016/j.ijhydene.2016.08.142.

[13] J. Li, M. Pan, H. Tang, Understanding short-side-chain perfluorinated sulfonic acid and its application for high temperature polymer electrolyte membrane fuel cells, RSC Adv. 4 (2014) 3944–3965. doi:10.1039/c3ra43735c.

[14] a. Stassi, I. Gatto, E. Passalacqua, V. Antonucci, a. S. Arico, L. Merlo, C. Oldani, E. Pagano, Performance comparison of long and short-side chain perfluorosulfonic membranes for high temperature polymer electrolyte membrane fuel cell operation, J. Power Sources. 196 (2011) 8925–8930. doi:10.1016/j.jpowsour.2010.12.084.

[15] I. Nicotera, V. Kosma, C. Simari, S. Angioni, P. Mustarelli, E. Quartarone, Ion dynamics and mechanical properties of sulfonated polybenzimidazole membranes for high-temperature proton exchange membrane fuel cells, J. Phys. Chem. C. 119 (2015) 9745–9753. doi:10.1021/acs.jpcc.5b01067.

[16] Z. Zuo, Y. Fu, A. Manthiram, Novel Blend Membranes Based on Acid-Base Interactions for Fuel Cells, Polymers (Basel). 4 (2012) 1627–1644. doi:10.3390/polym4041627.

[17] M.A. Hickner, H. Ghassemi, Y.S. Kim, B.R. Einsla, J.E. Mcgrath, Alternative Polymer Systems for Proton Exchange Membranes (PEMs), Chem. Rev. 104 (2004). doi:10.1021/cr020711a.

[18] J.A. Asensio, S. Borrós, P. Gómez-Romero, S. Borr, Enhanced conductivity in polyanion-containing polybenzimidazoles. Improved materials for proton-exchange membranes and PEM fuel cells, Electrochem. Commun. 5 (2003) 967–972. doi:10.1016/J.ELECOM.2003.09.007.

[19] M.Y. Kariduraganavar, A.A. Kittur, S.S. Kulkarni, Ion Exchange Membranes : Preparation , Properties , and Applications, 2012. doi:10.1007/978-94-007-1700-8.

[20] L. Wang, D. Wang, G. Zhu, J. Li, Synthesis and properties of highly branched sulfonated poly (arylene ether) s as proton exchange membranes, Eur. Polym. J. 47 (2011) 1985–1993. doi:10.1016/j.eurpolymj.2011.07.016.

[21] F. Lufrano, G. Squadrito, A. Patti, E. Passalacqua, Sulfonated Polysulfone as Promising Membranes for Polymer Electrolyte Fuel Cells, J. Appl. Polym. Sci. 77 (2000) 1250–1257.

[22] C. Simari, C. Lo Vecchio, A. Enotiadis, M. Davoli, V. Baglio, I. Nicotera, Toward optimization of a robust low-cost sulfonated-polyethersulfone containing layered double hydroxide for PEM fuel cells, J. Appl. Polym. Sci. 47884 (2019) 1–10. doi:10.1002/app.47884.

[23] D.W. Shin, S.Y. Lee, C.H. Lee, K.-S. Lee, C.H. Park, J.E. Mcgrath, M. Zhang, R.B. Moore, M.D. Lingwood, L.A. Madsen, Y.T. Kim, I. Hwang, Y.M. Lee, D. Won Shin, S. Young Lee, C. Hyun Lee, K.-S. Lee, C. Hoon Park, J. E. McGrath, M. Zhang, R. B. Moore, M. D. Lingwood, L. A. Madsen, Y. Taek Kim, I. Hwang, Y. Moo Lee, D.W. Shin, S.Y. Lee, C.H. Lee, K.-S. Lee, C.H. Park, J.E. Mcgrath, M. Zhang, R.B. Moore, M.D. Lingwood, L.A. Madsen, Y.T. Kim, I. Hwang, Y.M. Lee, Sulfonated Poly(arylene sulfide sulfone nitrile) Multiblock Copolymers with Ordered Morphology for Proton Exchange Membranes, Macromolecules. 46 (2013) 7797–7804. doi:10.1021/ma400889t.

[24] S. Zhong, X. Cui, H. Cai, T. Fu, C. Zhao, H. Na, Crosslinked sulfonated poly(ether ether ketone) proton exchange membranes for direct methanol fuel cell applications, J. Power Sources. 164 (2007) 65–72. doi:10.1016/J.JPOWSOUR.2006.10.077.

[25] S. Yang, Y. Ahn, D. Kim, Poly(arylene ether ketone) proton exchange membranes grafted with long aliphatic pendant sulfonated groups for vanadium redox flow batteries, J. Mater. Chem. A. 5 (2017) 2261–2270. doi:10.1039/C6TA07456A.

[26] C. Zhao, H. Lin, H. Na, Novel cross-linked sulfonated poly (arylene ether ketone) membranes for direct methanol fuel cell, Int. J. Hydrogen Energy. 35 (2010) 2176–2182. doi:10.1016/j.ijhydene.2009.12.149.

[27] V.B. Silva, V.S. Silva, L.M. Madeira, S.P. Nunes, A. Mendes, An impedance study on the sPEEK/ZrO 2 membranes for direct methanol fuel cell applications, Mater. Sci. Forum. 587–588 (2008) 926–930. doi:10.4028/www.scientific.net/msf.587-588.926.

[28] L.G. da Trindade, E.C. Pereira, SPEEK/Zeolite/Ionic-Liquid Anhydrous Polymer Membranes for Fuel-Cell Applications, Eur. J. Inorg. Chem. 2017 (2017) 2369–2376. doi:10.1002/ejic.201601559.

[29] C. de Bonis, C. Simari, V. Kosma, B. Mecheri, A. D'Epifanio, V. Allodi, G. Mariotto, S. Brutti, S. Suarez, K. Pilar, S. Greenbaum, S. Licoccia, I. Nicotera, Enhancement of proton mobility and mitigation of methanol crossover in sPEEK fuel cells by an organically modified titania nanofiller, J. Solid State Electrochem. 20 (2016). doi:10.1007/s10008-016-3167-x.

[30] C. Simari, G. Potsi, A. Policicchio, I. Perrotta, I. Nicotera, Clay-Carbon Nanotubes Hybrid Materials for Nanocomposite Membranes: Advantages of Branched Structure for Proton Transport under Low Humidity Conditions in PEMFCs, J. Phys. Chem. C. 120 (2016) 2574–2584. doi:10.1021/acs.jpcc.5b11871.

[31] H. Bai, H. Zhang, Y. He, J. Liu, B. Zhang, J. Wang, Enhanced proton conduction of chitosan membrane enabled by halloysite nanotubes bearing sulfonate polyelectrolyte

brushes, J. Memb. Sci. 454 (2014) 220–232. doi:10.1016/j.memsci.2013.12.005.

[32] Y. Kang, M. Obaid, J. Jang, M.H. Ham, I.S. Kim, Novel sulfonated graphene oxide incorporated polysulfone nanocomposite membranes for enhanced-performance in ultrafiltration process, Chemosphere. (2018). doi:10.1016/j.chemosphere.2018.05.141.

[33] A. Enotiadis, L.G. Boutsika, K. Spyrou, C. Simari, I. Nicotera, A facile approach to fabricating organosilica layered material with sulfonic groups as an efficient filler for polymer electrolyte nanocomposites, New J. Chem. 41 (2017) 9489–9496. doi:10.1039/c7nj01416c.

[34] W. Zhang, M.K.S. Li, P.-L. Yue, P. Gao, Exfoliated Pt-clay/Nafion nanocomposite membrane for self-humidifying polymer electrolyte fuel cells., Langmuir. 24 (2008) 2663–70. doi:10.1021/la702153v.

[35] I. Nicotera, A. Enotiadis, K. Angjeli, L. Coppola, D. Gournis, Evaluation of smectite clays as nanofillers for the synthesis of nanocomposite polymer electrolytes for fuel cell applications, Int. J. Hydrogen Energy. 37 (2012) 6236–6245. doi:10.1016/j.ijhydene.2011.06.041.

[36] Y. Zhu, A. Manthiram, Synthesis and characterization of polysulfone-containing sulfonated side chains for direct methanol fuel cells, J. Power Sources. 196 (2011) 7481–7487. doi:10.1016/j.jpowsour.2011.05.019.

[37] F. Trotta, E. Drioli, C. Moraglio, E. Baima Poma, Sulfonation of polyetheretherketone by chlorosulfuric acid, J. Appl. Polym. Sci. 70 (1998) 477–482. doi:10.1002/(SICI)1097-4628(19981017)70:3<477::AID-APP8>3.0.CO;2-K.

[38] F. Lufrano, V. Baglio, P. Staiti, A. Stassi, A.S. Aricò, V. Antonucci, Investigation of sulfonated polysulfone membranes as electrolyte in a passive-mode direct methanol fuel cell mini-stack, J. Power Sources. 195 (2010) 7727–7733. doi:10.1016/j.jpowsour.2009.11.130.

[39] S. Miyata, Anion-exchange properties of hydrotalcite-like compounds, in: Clay Clay Miner., 1983: pp. 305–311.

[40] F. Cavani, F. Trifirò, A. Vaccari, Hydrotalcite-type anionic clays: Preparation, properties and applications., Catal. Today. 11 (1991) 173–301. doi:10.1016/0920-5861(91)80068-K.

[41] G. Mishra, B. Dash, S. Pandey, Applied Clay Science Layered double hydroxides : A brief review from fundamentals to application as evolving biomaterials, Appl. Clay Sci. 153 (2018) 172–186. doi:10.1016/j.clay.2017.12.021.

[42] K. Lee, J.-H. Nam, J.H. Lee, Y. Lee, S.M. Cho, C.H. Jung, H.G. Choi, Y.-Y. Chang, Y.-U. Kwon, J.-D. Nam, Methanol and proton transport control by using layered double hydroxide nanoplatelets for direct methanol fuel cell, Electrochem. Commun. 7 (2005) 113–118.

doi:10.1016/J.ELECOM.2004.11.011.

[43] I. Nicotera, K. Angjeli, L. Coppola, A. Enotiadis, R. Pedicini, A. Carbone, D. Gournis, Composite polymer electrolyte membranes based on Mg–Al layered double hydroxide (LDH) platelets for H2/air-fed fuel cells, Solid State Ionics. 276 (2015) 40–46. doi:10.1016/j.ssi.2015.03.037.

[44] D.Y. Kim, E.H. Joo, A.K. Mishra, N.H. Kim, Y.J. Na, J.H. Lee, Synthesis and characterization of SPEEK/layered double hydroxide polymer nanocomposite for fuel cell applications, Adv. Mater. Res. 747 (2013) 234–237. doi:10.4028/www.scientific.net/AMR.747.234.

[45] M. Herrero, A.M. Martos, A. Varez, J.C. Galván, B. Levenfeld, Synthesis and characterization of polysulfone/layered double hydroxides nanocomposite membranes for fuel cell application, Int. J. Hydrogen Energy. 39 (2014) 4016–4022. doi:10.1016/j.ijhydene.2013.06.041.

[46] E. Lufrano, C. Simari, C. Lo Vecchio, A.S. Aricò, V. Baglio, I. Nicotera, Barrier properties of sulfonated polysulfone/layered double hydroxides nanocomposite membrane for direct methanol fuel cell operating at high methanol concentrations, Int. J. Hydrogen Energy. (2020). doi:10.1016/J.IJHYDENE.2020.02.101.

[47] J.F. Blanco, Q.T. Nguyen, P. Schaetzel, Sulfonation of polysulfones: Suitability of the sulfonated materials for asymmetric membrane preparation, J. Appl. Polym. Sci. 84 (2002) 2461–2473. doi:10.1002/app.10536.

[48] J.E. Tanner, Use of the stimulated echo in NMR diffusion studies, J. Chem Phys. 52 (1970) 2523–6.

[49] P. Cossari, C. Simari, A. Cannavale, G. Gigli, I. Nicotera, Advanced processing and characterization of Nafion electrolyte films for solid-state electrochromic devices fabricated at room temperature on single substrate, Solid State Ionics. 317 (2018). doi:10.1016/j.ssi.2017.12.029.

[50] N.S. Vasile, A.H.A. Monteverde Videla, C. Simari, I. Nicotera, S. Specchia, Influence of membrane-type and flow field design on methanol crossover on a single-cell DMFC: An experimental and multi-physics modeling study, Int. J. Hydrogen Energy. (2017). doi:10.1016/j.ijhydene.2017.06.214.

[51] V. Baglio, A. Stassi, F. V. Matera, V. Antonucci, A.S. Aricò, Investigation of passive DMFC mini-stacks at ambient temperature, Electrochim. Acta. 54 (2009) 2004–2009. doi:10.1016/j.electacta.2008.07.061.

[52] K. Angjeli, I. Nicotera, M. Baikousi, A. Enotiadis, D. Gournis, A. Saccà, E. Passalacqua, A.

Carbone, Investigation of layered double hydroxide (LDH) Nafion-based nanocomposite membranes for high temperature PEFCs, Energy Convers. Manag. 96 (2015) 39–46. doi:10.1016/j.enconman.2015.02.064.

[53] F.M. Uhl, S.P. Davuluri, S. Wong, D.C. Webster, Polymer Films Possessing Nanoreinforcements via Organically Modified Layered Silicate, Chem. Mater. 16 (2004) 4831–4838. doi:10.1021/cm035137d.

[54] P. Anadão, L.F. Sato, H. Wiebeck, F.R. Valenzuela-díaz, Montmorillonite as a component of polysulfone nanocomposite membranes, Appl. Clay Sci. 48 (2010) 127–132. doi:10.1016/j.clay.2009.12.011.

[55] D.H. Jung, S.Y. Cho, D.H. Peck, D.R. Shin, J.S. Kim, Preparation and performance of a Nafion®/montmorillonite nanocomposite membrane for direct methanol fuel cell, J. Power Sources. 118 (2003) 205–211. doi:10.1016/S0378-7753(03)00095-8.

[56] E. Lopez-Chavez, Y.Pena-Castaneda, G. Gonzalez-Garcıa, P. Perales-Enciso, A. Garcıa-Quiroz, J.I. Dıaz-Gongora, Theoretical methodology for calculating water uptake and ionic exchange capacity parameters of ionic exchange membranes with applications in fuel cells, Int. J. Hydrogen Energy. 40 (2015) 17316e17322 Available online at www.sciencedirect. doi:10.1016/j.ijhydene.2015.03.046.

[57] X.Q. Wang, C.X. Lin, F.H. Liu, L. Li, Q. Yang, Q.G. Zhang, Q.L. Liu, Alkali-stable partially fluorinated poly(arylene ether) anion exchange membranes with a claw-type head for fuel cells, J. Mater. Chem. A. 6 (2018) 12455–12465. doi:10.1039/c8ta03437k.

[58] I. Nicotera, C. Simari, L.G. Boutsika, L. Coppola, K. Spyrou, A. Enotiadis, NMR investigation on nanocomposite membranes based on organosilica layered materials bearing different functional groups for PEMFCs, Int. J. Hydrogen Energy. 42 (2017) 27940–27949. doi:10.1016/j.ijhydene.2017.05.014.

[59] I. Nicotera, V. Kosma, C. Simari, C. D'Urso, a. S. Aricò, V. Baglio, Methanol and proton transport in layered double hydroxide and smectite clay-based composites: influence on the electrochemical behavior of direct methanol fuel cells at intermediate temperatures, J. Solid State Electrochem. 19 (2015) 2053–2061. doi:10.1007/s10008-014-2701-y.

[60] C. Slichter, Principles of Magnetic Resonance, 3rd ed., New York, 1990.

[61] K.D. Kreuer, On the development of proton conducting polymer membranes for hydrogen and methanol fuel cells, J. Memb. Sci. 185 (2001) 29–39. http://linkinghub.elsevier.com/retrieve/pii/S0376738800006323.

[62] C. Felice, S. Ye, D. Qu, Nafion−Montmorillonite Nanocomposite Membrane for the Effective Reduction of Fuel Crossover, Ind. & Eng. Chem. Res. 49 (2010) 1514–1519.

doi:10.1021/ie901600a.

[63] C. Simari, V. Baglio, C. Lo Vecchio, A.S. Aricò, R.G. Agostino, L. Coppola, C. Oliviero Rossi, I. Nicotera, Reduced methanol crossover and enhanced proton transport in nanocomposite membranes based on clay−CNTs hybrid materials for direct methanol fuel cells, Ionics (Kiel). 23 (2017). doi:10.1007/s11581-017-2059-0.

[64] C. Simari, E. Lufrano, L. Coppola, I. Nicotera, Composite gel polymer electrolytes based on organo-modified nanoclays: Investigation on lithium-ion transport and mechanical properties, Membranes (Basel). 8 (2018). doi:10.3390/membranes8030069.

[65] Y. Kim, K. Ketpangr, S. Jaritphun, S. Park, S. Shanmugam, A polyoxometalate coupled graphene oxide–Nafion composite membrane for fuel cells operating at low relative humidity, J. Mater. Chem. A. 3 (2015) 8148–8155.

[66] M. Vinothkannan, A.R. Kim, G. Gnana Kumar, D.J. Yoo, Sulfonated graphene oxide/Nafion composite membranes for high temperature and low humidity proton exchange membrane fuel cells, RSC Adv. 8 (2018) 7494–7508. doi:10.1039/c7ra12768e.

[67] H.A. Patel, N. Mansor, S. Gadipelli, D.J.L. Brett, Z. Guo, Superacidity in Nafion/MOF Hybrid Membranes Retains Water at Low Humidity to Enhance Proton Conduction for Fuel Cells, ACS Appl. Mater. Interfaces. 8 (2016) 30687–30691. doi:10.1021/acsami.6b12240.